Supplemental Data for

Glycine Amidinotransferase (GATM), Renal Fanconi Syndrome, and Kidney Failure

Markus Reichold[#], Enriko D Klootwijk[#], Joerg Reinders[#], Edgar A Otto[#], Mario Milani, Carsten Broeker, Chris Laing, Julia Wiesner, Sulochana Devi, Weibin Zhou, Roland Schmitt, Ines Tegtmeier, Christina Sterner, Hannes Doellerer, Kathrin Renner, Peter J Oefner, Katja Dettmer, Johann M Simbuerger, Ralph Witzgall, Horia C Stanescu, Simona Dumitriu, Daniela Iancu, Vaksha Patel, Monika Mozere, Mehmet Tekman, Graciana Jaureguiberry, Naomi Issler, Anne Kesselheim, Stephen B Walsh, Daniel P Gale, Alexander J Howie, Joana R Martins, Andrew M Hall, Michael Kasgharian, Kevin O'Brien, Carlos R Ferreira, Paldeep S Atwal, Mahim Jain, Alexander Hammers, Geoffrey Charles-Edwards, Chi-Un Choe, Dirk Isbrandt, Alberto Cebrian-Serrano, Ben Davies, Richard N Sandford, Christopher Pugh, David S Konecki, Sue Povey, Detlef Bockenhauer, Uta Lichter-Konecki, William A Gahl[#], Robert J Unwin[#], Richard Warth[#]*, Robert Kleta[#]*

[#] *Contributed equally*
* *Corresponding authors*

Table of Contents

Supplemental Materials and Methods 3
- ^{1}H-NMR creatine spectroscopy 3
- Renal proximal tubular cell model 3
- RNA isolation 4
- Quantitative realtime PCR 4
- Immunofluorescence on inducible LLC-PK1 cells 5
- Analysis of plasma and urine of Gatm$^{+/+}$ and Gatm$^{-/-}$ mice 5
- Immunofluorescence on cryo sections 6
- Immunofluorescence on paraffin sections 6
- Masson-Goldner staining on paraffin sections 6
- Electron microscopy and immunogold labeling 6
- Quantification of intracellular IL-18 in inducible LLC-PK1 cells 7
- Determination of protein concentration with Bradford assay 7
- Measurement of extracellular LDH activity 7
- Live cell imaging of mitochondrial reactive oxygen species production 8
- Creatine supplementation 8
- Structural studies and data availability 9

Supplemental Figures 11
- Figure S1 11
- Figure S2 12
- Figure S3 13
- Figure S4 14
- Figure S5 15
- Figure S6 16
- Figure S7 17
- Figure S8 18
- Figure S9 20
- Figure S10 21

Supplemental Tables 22
- Table S1 22
- Table S2 22
- Table S3 23

References 24

Supplemental Materials and Methods

<u>^{1}H-NMR creatine spectroscopy</u>

^{1}H-NMR spectroscopy of body fluids shows the majority of proton-containing compounds and therefore can provide an overall view of metabolism.[1] ^{1}H-NMR spectrum provides a characteristic 'fingerprint' of almost all proton-containing metabolites. In these spectra, the spectral parameters chemical shift, spin-spin coupling, and signal intensity are important for body fluid analysis. The peak area or signal intensity of a resonance in a ^{1}H-NMR spectrum is proportional to the number of protons contributing to the signal when appropriate experimental conditions are used. Since the peak area is proportional to the number of protons contributing to the signal, it is also proportional to the concentration of the molecule concerned. Therefore, it is possible to use ^{1}H-NMR spectroscopy for metabolite quantification. The sensitivity of the technique is in the low micromolar range for most metabolites. It is well suited to detect creatine in urine, plasma, and cerebrospinal fluid as well as *in-vivo* within the brain (overview and details taken from [2]). Here, ^{1}H-NMR spectra were acquired on an Achieva 3T MR scanner (Philips, Best, The Netherlands) using a PRESS sequence (TR=2000 ms, TE=35 ms, 128 averages, 15x15x15 mm voxel) and processed in LCModel (Provencher, Magn Reson Med 30, 672 (1993)), referencing to the unsuppressed water.

<u>Renal proximal tubular cell model</u>

A permanently transfected, inducible renal proximal tubular cell line derived from LLC-PK1 cells was created for each patient GATM mutation using recombinant technology. LLC-PK1 cells are an established model and reliably express many properties of the renal proximal tubule.[3] We previously had established tetracycline-inducible stable transfected LLC-PK1 cells that were obtained using the Flp-in T-Rex system (Invitrogen, Paisley, UK) containing the constructs pFRT/lacZeo and pcDNA/5/TR (JCRB0060, Health Science Research Resources Bank, Tokyo, Japan). These cell lines and derived cells were maintained in 1 g/L glucose DMEM (PAA laboratories, E15-005, Yeovil, UK) medium with 8% fetal bovine serum (PAA laboratories, A15-109, Yeovil, UK), 2 mM L-glutamine (PAA laboratories, M11-006, Yeovil, UK), penicillin (100 U/ml)/streptomycin (100 µg/ml) (PAA laboratories, P11-010, Yeovil, UK).

The human *GATM* coding region was obtained from a Trueclone full length cDNA clone (sc321307, NM_001482.1; Origene Technologies; Rockville, MD, USA). The Origene vector containing the full length *GATM* cDNA was subcloned into the *NotI* site of the pcDNA5FRT/TO vector. The patients' mutations c.958C>T (p.P320S), c.1006A>G (p.T336A), c.1007C>T (p.T336I), and c.1022C>T (p.P341L), were inserted via site-directed mutagenesis (QuikChange II, Stratagene, Santa Clara, CA USA). To this end the following oligo pairs were used:

5'-GTATTGTGCTTTCCAAC**<u>T</u>**CTGACCGACCATGTCAC-3',
5'-GTGACATGGTCGGTCAGAGTTGGAAAGCACAATAC-3' (c.958C>T);
5'-TCAAGAAAGCAGGATGG**<u>G</u>**CTATCATTACTCCTC-3',
5'-GAGGAGTAATGATAG**<u>C</u>**CCATCCTGCTTTCTTGA-3' (c.1006A>G);
5'-TCAAGAAAGCAGGATGGA**<u>T</u>**TATCATTACTCCTC-3',
5'-GAGGAGTAATGATA**<u>A</u>**TCCATCCTGCTTTCTTGA-3' (c.1007C>T);
5'-TCAAGAAAGCAGGATGGA**<u>T</u>**TATCATTACTCCTCC-3',
5'-GGAGGAGTAATGATA**<u>A</u>**TCCATCCTGCTTTCTTGA-3' (c.1022C>T).

The full length wildtype and mutant cDNA clones were all sequence-verified. The stable transfected Frt-1 cells containing the pcDNA/5/TR construct were cotransfected at a ratio of 9:1 (w/w) circularized pOG44:pcDNA5/FRT/TO/GATM, pOG44:pcDNA5/FRT/TO/T336AGATM, pOG44:pcDNA5/FRT/TO/T336IGATM, pOG44:pcDNA5/FRT/TO/P341LGATM, or pOG44:pcDNA5/FRT/TO/P320SGATM. Transfection was performed using lipofectamine 2000 (Thermofisher Scientific, 11668027, UK) according to the protocol of the manufacturer. The transfected cells were incubated for four weeks in selection medium containing 500 µg/ml hygromycin-B. Several clones were obtained for cells transfected with these constructs. Incorporation of the constructs in the genomic DNA was demonstrated by PCR analysis, and subsequently sequence analysis of the full coding region of human *GATM*. These PCR and sequence conditions are available on request. Induced expression of human *GATM* was achieved using 1 µg/ml tetracycline (Applichem/VWR, A1685, Lutterworth, UK) for each of the clones. To this end, real-time PCR (conditions used available on request), Western analysis (conditions used available on request) and immunohistochemical analysis were utilized. For all functional analyses described, a single clone was used. Upon induction with 1 µg/ml tetracycline these clones showed equal expression of human *GATM*.

RNA isolation

Inducible LLC-PK1 cells were seeded in cell medium (RPMI medium 1640 with 11.1 mM glucose (Gibco Cell Culture Systems - Invitrogen, Karlsruhe, Germany), FCS 10%, penicillin G 5 I.U., streptomycin 50 µg/ml, sodium hexanoate 5 mM). To induce the expression system of the cells, tetracycline (1 µg/ml) was added to the medium. Cells were cultured and induced for three weeks until RNA was isolated. Medium was changed every other day. Total RNA from inducible LLC-PK1 cells was isolated using a column based kit optimized for the purification from small amounts of tissue according to the manual (RNeasy Micro Kit, Qiagen, Hilden, Germany). The RNA concentration was quantified with a photometer (NanoDrop ND-1000, PEQLAB Biotechnologie GmbH, Erlangen, Germany). Quality of the RNA used for real-time RT-PCR was tested by agarose electrophoresis.

Quantitative realtime PCR

Reverse transcription with M-MLV-RT (Promega GmbH, Mannheim, Germany) and random primers (Fermentas GmbH, St. Leon-Rot, Germany) was done using 1 µg total RNA to generate single-stranded cDNA. Relevant contamination with genomic DNA was excluded by negative control reactions without the reverse transcriptase enzyme (-RT). Realtime PCR of cDNA samples was performed on a LightCycler 480 device (Roche, Basel, Switzerland) using specific and, wherever applicable, intron-spanning primers, and a SYBR® Green mastermix (Roche, Basel, Switzerland). Target gene expression levels were quantified relative to beta-actin expression under consideration of PCR efficiencies calculated on the basis of standard dilution curves. The specificity of PCR amplifications was verified by agarose electrophoresis and melting curve analysis. Primer sequences (Life Technologies GmbH, Darmstadt, Germany) are listed in Supplemental Table S2.

For realtime-PCR experiments in LLC-PK1 cells (porcine NLRP3, porcine IL-18, porcine FN1, porcine ACTA2, Fig. 3J, K and Fig. 4A, B), n=20 petri dishes of three independent experimental series were used (each series with vector control cells and cells over-expressing wildtype GATM or the T336A mutant). For realtime PCR experiments determining the murine GATM expression in mouse kidneys after a high creatine diet, n=4 treated and n=4 untreated animals were used. Data are shown as mean values ± standard error of the mean (SEM); “n” stands for the number of observations. ANOVA followed by a Bonferroni Test (OriginPro, Northampton, MA 01060, USA) (Fig. 3J, K and Fig. 4A, B)

or *t*-test (Fig. 4E) were used to determine statistical significance. A p-value of 0.05 was accepted to indicate statistical significance.

Immunofluorescence on inducible LLC-PK1 cells

Inducible LLC-PK1 cells were grown on glass coverslips and induced with tetracycline (1 µg/ml) for at least 24 h. For mitochondrial staining, MitoTracker Orange CMTMRos (Invitrogen, Karlsruhe, Germany) was added (1:5000) to the medium and incubated at 37℃, 5% CO_2, for 30 min. After washing with Ringer's solution, cells were fixated for 15 min with 3% paraformaldehyde in PBS (phosphate buffered saline pH 7.4). Cells were rinsed twice with PBS and afterwards incubated in PBS containing 0.1% SDS for 5 min to unmask the epitopes followed by another wash with PBS for 2 x 5 min. Primary antibodies were applied for 1 h. Primary and secondary antibodies were diluted in PBS with 0.04% Triton X-100 (Sigma, Taufkirchen, Germany). After washing twice (PBS, 5 min), cells were incubated for 1 h with the secondary antibody and HOE33342 to stain the nuclei. After a final washing step (PBS, 2 x 5 min), the glass coverslips with the cells were mounted on slides with fluorescent-free glycergel mounting medium (DakoCytomation, Hamburg, Germany). A list of all used primary and secondary antibodies as well as further dyes is provided in Supplemental Table S3.

Analysis of plasma and urine of $Gatm^{+/+}$ and $Gatm^{-/-}$ mice

Spot urine of 9 - 12 week old $Gatm^{+/+}$ (n=6) and $Gatm^{-/-}$ (n=6) mice was collected twice per mouse on two different days. After the last sample was taken, mice were sacrificed and blood was collected. Metabolites of the creatine synthesis pathway (creatinine, creatine, guanidinoacetate), blood glucose, and amino acids were measured in urine and plasma. All urine values were normalized to urinary osmolality. For measurements urine samples were diluted 1:4. Amino acids were derivatized with propylchloroformate/propanol and measured by LC-MS/MS with electrospray ionization in positive mode and detection by multiple reaction monitoring (MRM) as recently described.[4] 5 µl of diluted urine or plasma were used for derivatization. Quantification was based on calibration curves using ^{13}C,^{15}N-labeled amino acids as internal standards.
Creatinine, creatine, and guanidinoacetate were analyzed by LC-MS/MS with electrospray ionization (ESI) in positive mode. An Agilent 1200 SL HPLC hyphenated to an AB Sciex (Darmstadt, Germany) 4000 QTrap mass spectrometer working with a TurboV electrospray ion source was used. HPLC separation was performed on an Atlantis T3 reversed-phase column (150 mm × 2.1 mm i.d., 3 µm, Waters, Eschborn, Germany) with mobile phases A (0.1% formic acid in water, v/v) and B (0.1% formic acid in acetonitrile, v/v) employing a flow rate of 350 µl/min. The following gradient was used with deviating parameters for the positive mode ionization run given in brackets: 0–10 min linear increase from 0% to 100% B, hold for 2 min (0 min) and return to 0% B at 12.1 min (10.1 min) and equilibrate for 7 min. The column was kept at 25℃. An injection volume of 10 µl was used. Analytes were detected in MRM mode. For the analysis in positive mode ionization, two time segments were programmed detecting different analytes. Quantification was based on calibration curves using the stable isotope-labelled analogues as internal standards. Creatinine-d3 was used as internal standard for creatine and guanidinoacetate, because they eluted close to each other.

10 µl internal standard (IS1) solution, containing creatinine-d3 at a concentration of 100 µM, were added to 10 µl pre-diluted urine and further diluted with water to a final volume of 100 µl. A plasma aliquot of 25 µl was spiked with 5 µl IS1 solution and 10 µl surrogate solution containing [U-^{13}C]glucose, [U-^{13}C]lactic acid, and [U-^{13}C]pyruvic acid at a concentration of 1 mM. Proteins were precipitated with 150 µl cold methanol and samples were centrifuged for 5 min at 4℃ and 11200 g. The supernatant was collected

and dried using a vacuum evaporator (CombiDancer, Hettich AG, Bäch, Switzerland). The residue was redissolved in 100 µl water and subjected to analysis.

p-values for urine analysis: Creatinine = 0.0002, Creatine = 0.0140, Guanidinoacetate = 0.0001. p-values for plasma analysis: Creatinine = 0.0026, Creatine = 0.0010, Lactate = 0.0031, Serine = 0.0021, Threonine = 0.0017. Data are shown in mean values ± standard error of the mean (SEM); "n" stands for the number of observations. An unpaired *t*-test was used to determine statistical significance. As multiple parameters were tested in urine and plasma, p-values were corrected according to Bonferroni correction (0.05/ n). p-values of 0.0167 (metabolites of the creatine pathway), 0.0167 (metabolites of the energy pathway), and 0.0025 (amino acids) were accepted to indicate statistical significance.

Immunofluorescence on cryo sections

Cryosections (5 µm) were mounted on poly-L-lysine slides (Kindler, Freiburg, Germany). Prior to incubation with the primary antibodies, sections were incubated in 0.1% SDS (5 min) for unmasking of epitopes, washed in PBS (2 x 5 min) followed by blocking with 5% bovine albumin (10 min). Primary and secondary antibodies were diluted in phosphate buffered saline (PBS), pH 7.4, with 0.04% Triton X-100 (Sigma, Taufkirchen, Germany). Primary antibodies were applied overnight at 4℃. After washing with PBS (2 x 5 min), sections were incubated for 1 h with the secondary antibodies and HOE33342 to stain the nuclei. The slides were then washed in PBS (2 x 5 min) and mounted with fluorescent-free glycergel mounting medium (DakoCytomation, Hamburg, Germany). A list of all used primary and secondary antibodies as well as further dyes is provided in Table S3.

Immunofluorescence on paraffin sections

Human kidney samples were embedded in paraffin and slices (5 µm) were mounted on poly-L-lysine slides (Kindler, Freiburg, Germany). To remove paraffin from the tissues, slides were put into xylol twice for 10 min each and afterwards rehydrated in an alcohol series (99% isopropanol, 95% EtOH, 80% EtOH, 70% EtOH) for 10 min each. Then, slices were rinsed with PBS for 5 min and heated at 95℃ i n citrate buffer (pH 6.0) for 15 min to unmask epitopes. The rest of the protocol was performed according to the protocol for cryosections. A list of all used primary and secondary antibodies as well as further dyes is provided in Table S3.

Masson-Goldner staining on paraffin sections

For Masson-Goldner staining, sections were deparaffinized as described above. Afterwards, slices were incubated in Weigert's Iron Hematoxylin solution for 2 min, rinsed in running tap water for 2 min and then briefly put into 0.1% HCl-alcohol solution. Subsequently, the slices were rinsed in running tap water for 10 min, incubated in 0.5% phosphor tungistic acid for 15 sec and washed three times for 5 min each in distilled water, before they were stained in fuchsine acid and Ponceau for 10 min. Next, slides were incubated 3 times each for 1 min in 1% glacial ethanoic acid, 20 sec in orange G-solution, 2 min in 1% glacial ethanoic acid, 4 min in lightgreen-solution and rinsed twice in 2% glacial ethanoic acid. Afterwards, slices were dehydrated in 96% isopropanol (20 sec), 99% isopropanol (twice for 5 min each) and xylol (twice for 10 min each). The slides were mounted with xylol-containing DEPEX-medium.

Electron microscopy and immunogold labeling

Kidney specimens of our Fanconi patients were originally embedded in paraffin. For electron microscopy, samples were deparaffinized according to the following protocol:

xylol (2 x 15 min, 3 x 30 min), 100% ethanol (5 x 15 min), 95% ethanol (15 min), 90% ethanol (15 min), 70% ethanol (15 min), 50 % ethanol (15 min), distilled water (2 x 15 min). After post fixation with 4% glutaraldehyde solution (in 0.1 M Na-cacodylate pH 7.4 for 60 min) samples were finally rinsed with 0.1 M Na-cacodylate pH 7.4 (2 x 15 min).

Inducible LLC-PK1 cells were grown on cover slips and induced with tetracycline (1 µg/ml) for 3 d. Before embedding, cells were fixed using a 2% glutaraldehyde solution in 0.1 M Na-cacodylate pH 7.4 for about 1 h. Post fixation and dehydration of the samples was carried out using the following protocol: rinsing in 0.1 M Na-cacodylate pH 7.4 (3 x 20 min), 1% OsO4 in 0.1 M Na-cacodylate pH 7.4 (2 h), 0.1 M Na-cacodylate pH 7.4 cacodylic acid (3 x 20 min), 50% ethanol (15 min), 70% ethanol (15 min), 90% ethanol (15 min), 96% ethanol (15 min), 100% ethanol (20 min), acetone (3 x 15 min). Finally, samples were embedded in Epon and polymerized at 60℃ for 48 h using standard protocols. For immunogold labeling, freshly prepared ultrathin sections (70 nm; Ultracut UC6; Leica, Wetzlar, Germany) were mounted on grids and treated according to the following protocol: 0.1% glycine in PBS (5 min), 1% BSA in glycine solution (5 min), primary antibody against GATM in 0.1% BSA in PBS for 1.5 h, 0.1% BSA in PBS (5 x 2 min), secondary antibody (goat anti rabbit 6 nm gold particles; Aurion, Wageningen, Netherlands) in 0.1% BSA in PBS for 1.5 h, 0.1% BSA in PBS (5 x 2 min), PBS (2 x 2 min), 2% glutaraldehyde in PBS (5 min), PBS (2 x 2 min), distilled water (3 x 2 min). To improve contrast, specimens were stained with 2% UAc for 30 min. Ultrathin sections were imaged using either an EM902 (Zeiss, Oberkochen, Germany) or a JEM-2100F (JEOL, Tokyo, Japan) transmission electron microscope, operated at 80keV (902) or 200 keV (JEM). Digital micrographs were recorded using a CCD 2k camera (Troendle, Moorenweis, Germany) or a CMOS 4k F416 camera (TVIPS, Gauting, Germany).

Quantification of intracellular IL-18 in inducible LLC-PK1 cells

Quantification of intracellular IL-18 protein content in induced LLC-PK1 cells was performed using an ELISA Kit form PromoKine (PK-EL-62816P, Heidelberg, Germany) recognizing porcine IL-18. The ELISA was performed according to the manufacturer's protocol. n =3 petri dishes were used for LLC-PK1 cells over-expressing the wildtype protein or the T336A mutant, respectively. Cells were induced with tetracycline for 2 weeks. In the following week, tetracycline was removed from the medium. After 3 weeks, cells were lysed and intracellular content of IL-18 was quantified. Data were normalized to total protein content determined by Bradford assay. p-value = 0.0012. Data are shown as mean values ± standard error of the mean (SEM); "n" stands for the number of observations. An unpaired *t*-test was used to determine statistical significance and a p-value of 0.05 was accepted to indicate statistical significance.

Determination of protein concentration with Bradford assay

Frozen cell pellets were used to determine protein concentration of inducible LLC-PK1 cells. Cell pellets were resuspended in sample buffer containing DTT, 86% glycerol, 10 % SDS, 0.5 M tris(hydroxymethyl)aminomethane (TRIS) pH 6.8, 0.5 M $MgCl_2$, and 25 U/µl benzonase. For quantification, different BSA solutions of known concentration were prepared. All samples were diluted in Bradford reagent (1:100) and transferred to a 96-well plate. After incubating for 15 min in the dark, the absorption at 595 nm was measured in a microplate reader (Bio-Rad, Hercules, USA). Protein concentrations were determined on the basis of the standard linear slope from the BSA standards.

Measurement of extracellular LDH activity

For over-expression of wildtype GATM or T336A mutant proteins, respective LLC-PK1 cells were induced with tetracycline for 3 weeks (plus the days shown on the x-axis

in the graph of Fig. 4C). Extracellular LDH activity as a surrogate marker of cytolysis was measured using Pierce™ LDH cytotoxicity assay kit (Thermo Fisher Scientific, Bonn, Germany). The experiments were carried out in triplicate and normalized to the total cellular protein amounts determined by Bradford assay. Significant differences were determined in IBM SPSS 23 using two-way ANOVA with post-hoc Student´s *t*-tests corrected for multiple testing by the Bonferroni method (0.05/n = 0.0167). p-values were 0.0039 (day 2), <0.0001 (day 3), and <0.0001 (day 4). Data are shown as mean values ± standard error of the mean (SEM); "n" stands for the number of observations.

Live cell imaging of mitochondrial reactive oxygen species production

$3.5x10^5$ LLC-PK1 cells were seeded on a 30-mm cover glass coated with poly-L-lysine. When confluent, cells were incubated with 1 µg/ml tetracycline for 48 h to induce expression of wildtype- or mutant T336A GATM. Reactive oxygen species (ROS) production was measured by incubating the cells with 5 µM CellROX Deep Red (Life Technologies) for 30 min at 37℃. The rate of incre ase in fluorescence signal was taken as proportional to the rate of ROS production. Cells were imaged at 37℃ using a Leica SP5 automated inverted confocal laser scanning microscope and a 63x objective. CellROX was excited at 633 nm and light was collected between 638 nm and 737 nm. Images were acquired every 10 min to minimize laser-induced photo-toxicity for a maximal duration of 40 min. 7 coverslips of induced wildtype and 6 of mutant T336A GATM were imaged. 30 fields were acquired per coverslip using the Matrix screener Leica software and normalized to the initial fluorescence after incubation (30 min with CellROX). Images were analyzed using Image J software (https://imagej.nih.gov/ij/). The results are presented as mean values ± SEM. Statistical analysis was performed using Prism 6 (http://www.graphpad.com) by comparing the rates of ROS production between wildtype and mutant cells using a linear regression analysis (equivalent to analysis of covariance (ANCOVA)).

Creatine supplementation

Male, wildtype C57Bl/6 mice (n=8, age 10 weeks, Jackson Laboratories) were randomly assigned to either a group nourished with a diet consisting of bread and tap water (low creatine, high carbohydrate diet) or a group with an additional supplement of 1% (w/w) creatine (Sigma-Aldrich Chemie GmbH, Steinheim, Germany) in the drinking water. After sacrificing the mice kidneys were removed, divided into halves, then immediately frozen in liquid nitrogen and stored at -80℃ until further experimentation. Frozen mouse kidneys were pulverized in liquid nitrogen using a mortar and RNA was isolated using RNeasy Mini Kit (Qiagen GmbH, Hilden, Germany) according to the manufacturer's recommendations. RNA was quantified using the NanoDrop 2000c spectrophotometer (Peqlab Biotechnologie GmbH, Erlangen, Germany) and its quality was assessed by imaging on 1% agarose gel. RNA was then transcribed to cDNA using Reverse Transcription System (Promega, Madison, WI) according to the manufacturer's recommendations. Real-time PCR was performed as described above using cDNA, SYBR® Green mix (Roche Diagnostics GmbH, Mannheim, Germany) and primers for mouse Gatm or β-actin (Table S4). For real-time PCR, a Light Cycler 480 (Roche Diagnostics, Rotkreuz, Switzerland) was employed according to the manufacturer's recommendations. Quality and size of the amplicon were further verified by visualization on 3% agarose gels.

Frozen mouse kidneys were weighed, then pulverized in liquid nitrogen using a mortar and proteins eluted by incubation in 3 µl/mg kidney tissue of a lysis-buffer containing RIPA-buffer (1% Igepal CA-630, 0.5% sodium-desoxycholate, 0.1% SDS in PBS), 200 mM PMSF (1/200 v/v) and EDTA-free protease inhibitor cocktail set III (1/100

v/v, Calbiochem, San Diego, CA) for 20 min on ice. Samples were centrifuged at 14.800 rpm for 10 min at 4℃ and supernatants stored at -2 0℃ until further analysis. The protein content of the samples was quantified in 96-well plates (Nuncleon Delta Surface, NUNC A/S, Roskilde, Denmark) according to Bradford using Bio-Rad protein assay (Bio-Rad Laboratories GmbH, Muenchen, Germany) and Bio-Rad 550 Microplate Reader (Bio-Rad) according to the manufacturer's recommendations. Equal amounts of proteins in Laemmli-buffer (Bio-Rad) including 2-mercaptoethanol 1/20 (v/v, Merck Schuchard, Hohenbrunn, Germany) were cooked for 5 min, separated by 10% SDS-PAGE and transferred to a PVDF blotting membrane (Amersham Hybond). The membrane was blocked by incubation with 5% fat-free dry milk-powder (w/v, AppliChem GmbH, Darmstadt, Germany) in PBS-Tween for 1 h at room temperature followed by incubation with primary antibody polyclonal rabbit anti-GATM (1/2000 v/v, Proteintech, Manchester, UK) in 1.5% BSA in PBS-Tween at 4°C overnight. The secondary antibody donkey anti-rabbit IgG-horseradish peroxidase (HRP, 1/5000, v/v, Santo Cruz Biotechnology) in 1% PBS-Tween was incubated for 1 h at room temperature and protein bands developed using Western Blot Luminol Reagent (Santa Cruz Biotechnology, Heidelberg, Germany) and visualized in Fusion Fx7 (Vilber Lourmat, Marne-la-Vallee, France). The membranes were stripped from bound antibodies by applying Restore Western Blot Stripping Buffer (Thermo Scientific, Rockford, IL) for 15 min at room temperature, washed, blocked as described above and the house-keeping protein was detected using as primary antibody rabbit anti-mouse beta-actin (1/5000 v/v, Sigma-Aldrich, Taufkirchen, Germany) in 1.5% BSA-PBS-Tween at 4℃ overnight and as secondary antibody do nkey anti-rabbit IgG-HRP (1/5000, v/v, Santa Cruz Biotechnology, Heidelberg, Germany) in 1% PBS-Tween for 1 h at room temperature. Quantification of Gatm and beta-actin was performed with ImageJ.

p-values: RT-PCR = 0.0125, Western blot quantification = 0.029 . Data are shown in mean values ± standard error of the mean (SEM); "n" stands for the number of observations. An unpaired *t*-test was used to determine statistical significance and a p-value of 0.05 was accepted to indicate statistical significance.

Structural studies and data availability

To test the hypothesis of mutation-mediated aggregation of GATM, we performed molecular dynamics simulations on the wildtype monomer and on the four mutants. Modelling of possible protein-protein interaction surfaces (GRAMM-X; http://vakser.bioinformatics.ku.edu/resources/gramm/grammx/) started with the structure of the wildtype monomer (pdb: 1JDW at http://www.rcsb.org/pdb/home/home.do).

We utilized publicly available GATM crystal structures (i.e. 1JDW subunit A) to simulate the effect of all mutations recognized in our patients. In order to test the hypothesis of mutation-mediated destabilization of the region around B4, we performed molecular dynamics simulations on the wildtype monomer and on the four mutants, starting from the coordinates of 1JDW subunit A. Each simulation lasted for 40 ns. At the end of the simulations (after 40 ns) superposing all the mutants on the wildtype protein results in Cα root mean square displacement (r.m.s.d.) from 1.12 to 1.47 Å (from 1.17 to 1.72 Å if we limit the superposition on the region around the B4 surface). The lower differences with respect to the wildtype in T336A mutant could be related to the fact that this mutation may require more time (with respect to the 40 ns of the simulation) to propagate its effect.

In order to test the possibility of stable dimerization based on the B4 surface, we performed two additional molecular dynamics simulations on the wildtype and on the P341L B4-based dimers as modelled by the program GRAMM-X. The P341L mutant was chosen being the one with the higher overall r.m.s.d. respect to wildtype GATM during the previous simulations, therefore the most variable during the simulation time.

Along the simulation, the wildtype dimer analyzed by the program PISA (www.ebi.ac.uk/pdbe/pisa/) adopts different configurations compatible with stable and unstable dimeric assemblies. Interestingly, the P341L dimer promptly evolves toward stability (after 10 ns) that is maintained along the remaining simulation time. Such simulation results show, on one hand, how the B4 interface is prone to protein-protein interaction also in the wildtype protein and, on the other hand, how it is sufficient for only a point mutation (P341L) to shift the B4 based monomer-dimer equilibrium towards another stable quaternary assembly. This analysis, as the one shown before, clearly supports the hypothesis that the mutation induced structural rearrangements of the B4 surface do promote a new protein-protein interaction surface that can lead to linear aggregation of GATM.

For cell expression studies, the human GATM coding region obtained from a Trueclone full length cDNA clone (sc321307, https://www.ncbi.nlm.nih.gov/nuccore/NM_001482.1; Origene Technologies; Rockville, MD, USA) was used.

Supplemental Figures

Figure S1

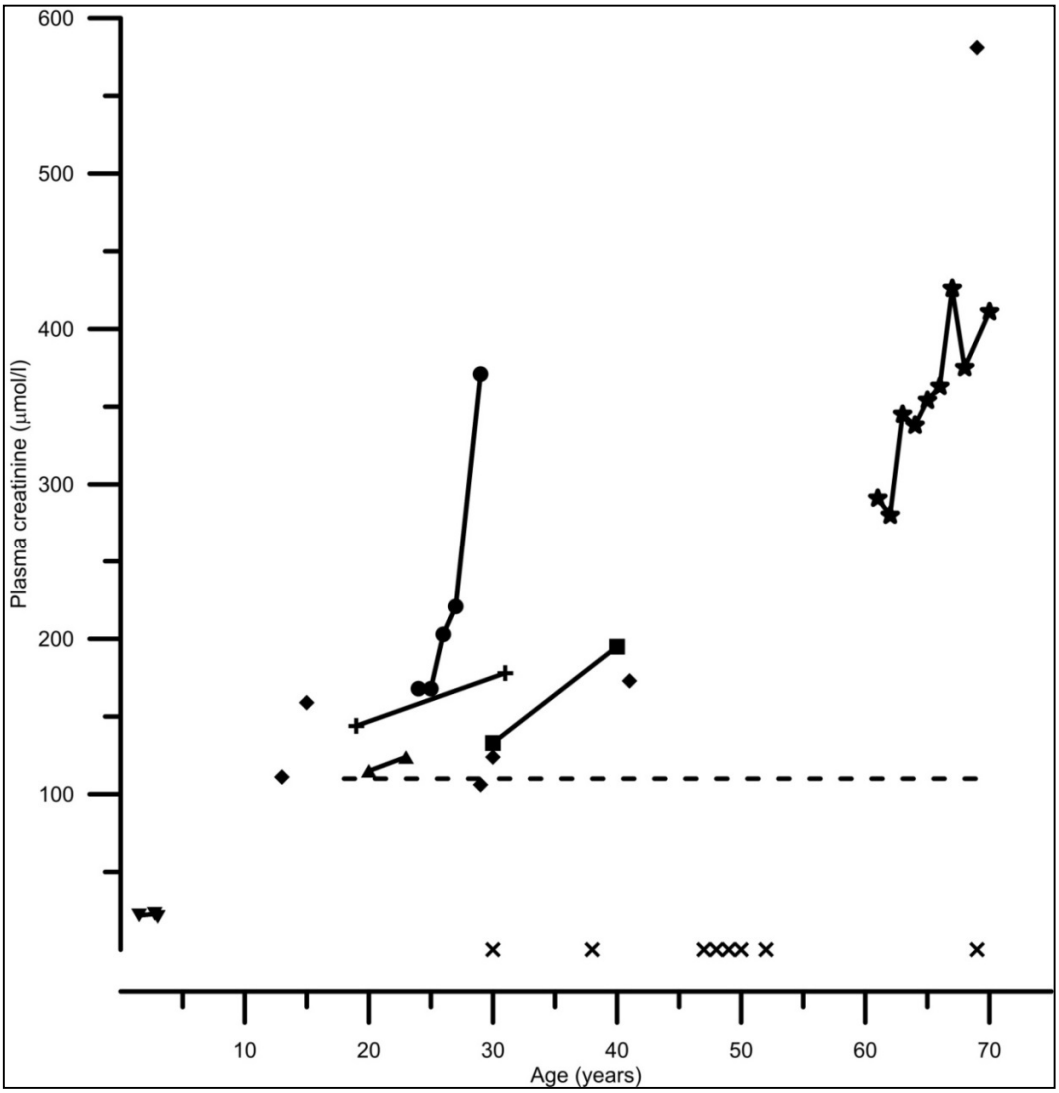

Graph illustrating decline in kidney function in GATM related renal Fanconi syndrome and kidney failure and age at kidney transplantation. Data from affected and genotyped individuals are shown. In six individuals (▼, ✚, ▲, ●, ■, ★) connecting lines indicate serial measurements. In another six individuals (◆) single creatinine measurements are plotted. In eight individuals (✖) age at kidney transplantation is presented. The horizontal dashed line indicates normal plasma creatinine (110 µmol/l) for an average adult person. Note normal plasma creatinine in the youngest child and ensuing kidney failure in individuals from adolescence on with need for transplant as early as 30 years of age.

Figure S2

```
                P320S          T336A/I P341L
                 ↓                 ↓    ↓
Homo            NPDRPCHQIDLFKKAGWTIITPPT
Pan             NPDRPCHQIDLFKKAGWTIITPPT
Macaca          NPDRPCHQIDLFKKAGWTIITPPT
Otolemur        NPDRPCHQIDLFKKAGWTIVTPPT
Rattus          NPDRPCHQIDLFKKAGWTIVTPPT
Mus             NPDRPCHQIDLFKKAGWTIVTPPT
Cavia           NPDRPCHQIDLFKKAGWTIVTPPT
Oryctolagus     NPDRPCLQIELFKKAGWTIVTPPI
Sorex           NPDRPCHQIDLFKKAGWTIVTPPI
Canis           NPDRPCHQIDLFKKAGWTIVTPPI
Felis           NPDRPCHQIDLFKKAGWTIVTPPI
Equus           NPDRPCHQIDLFKKAGWTIVTPPI
Bos             NPDRPCHQIDLFKKAGWTIVTPPT
Dasypus         NPDRPCHQIDLFKKAGWTIVTPPI
Echinops        NPDRPCHQVDLFKKAGWTIVIPPK
Monodelphis     NPDRPCHQIELFKKAGWTIVTPPT
Gallus          NPDRPCHQIELFKKAGWTVIHPPV
Xenopus         NPDRPCHQIELFKKAGWTVVTPPT
```

Protein alignment plot. Protein alignment (homology) plot of the mutations bearing non-catalytical region of GATM (amino acids 319-342) in 18 vertebrate species. Note complete conservation of the amino acids (i.e. mutations: P320S, T336A, T336I, P341L) identified (indicated by arrows and letters in red).

Figure S3

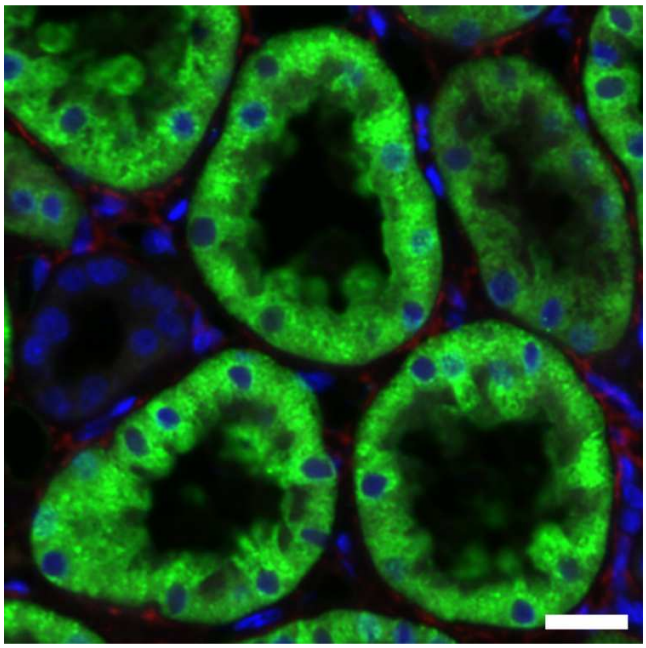

Control staining for Fig. 1E. Immunofluorescence of a kidney specimen of a healthy control person. GATM is labeled green, α-smooth muscle actin (a marker for myofibroblasts) red, and nuclei blue. Compared to the renal Fanconi and kidney failure patient's post mortem kidney specimen shown in Fig. 1E, there is almost no α-smooth muscle actin staining detectable. There is no obvious difference in expression levels of GATM between control and patient. Scale bar: 20 µm.

Figure S4

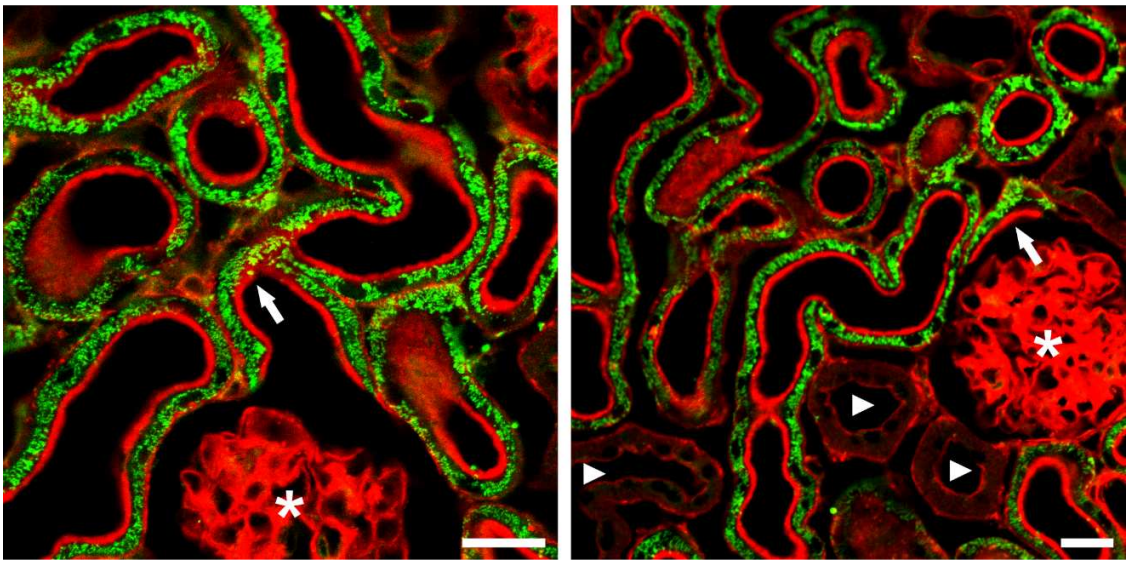

Immunofluorescence of Gatm in mouse kidney: Gatm expression (green) starts at the early proximal tubule right at the urinary pole (arrows) of the glomerulus (asterisks) and decreases towards the late segments of the proximal tubule. F-actin (red) was used as a marker for the proximal tubular brush border. Note, non-proximal nephron segments (arrow heads) including the glomeruli (asterisks) do not show any Gatm expression. Scale bars: 20 µm.

Figure S5

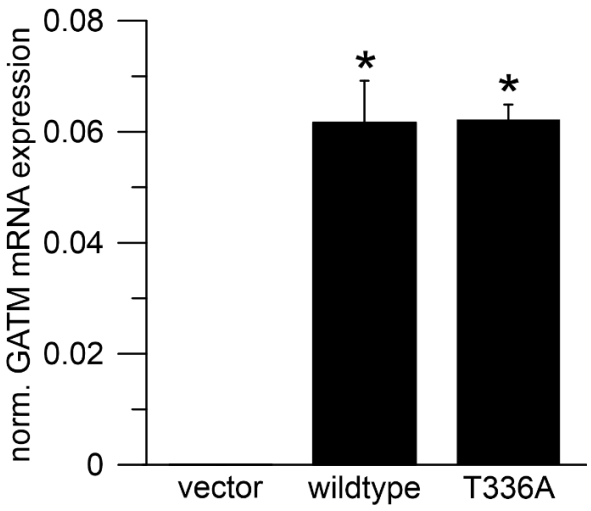

Expression levels of human GATM mRNA in the inducible LLC-PK1 model. After inducing GATM expression with tetracycline, expression levels of wildtype GATM and the mutant form T336A were very similar. “Vector” cells contained the empty Flp-in T-Rex system. With the primers for human GATM used here, endogenous expression of porcine Gatm could not be detected. * significantly different from vector control cells (ANOVA, Bonferroni test, n = 3 per group, vec vs. wt: p = 0,00024, vec vs. T336A: p = 0,00023, wt vs. T336A: p = 1,0)

Figure S6

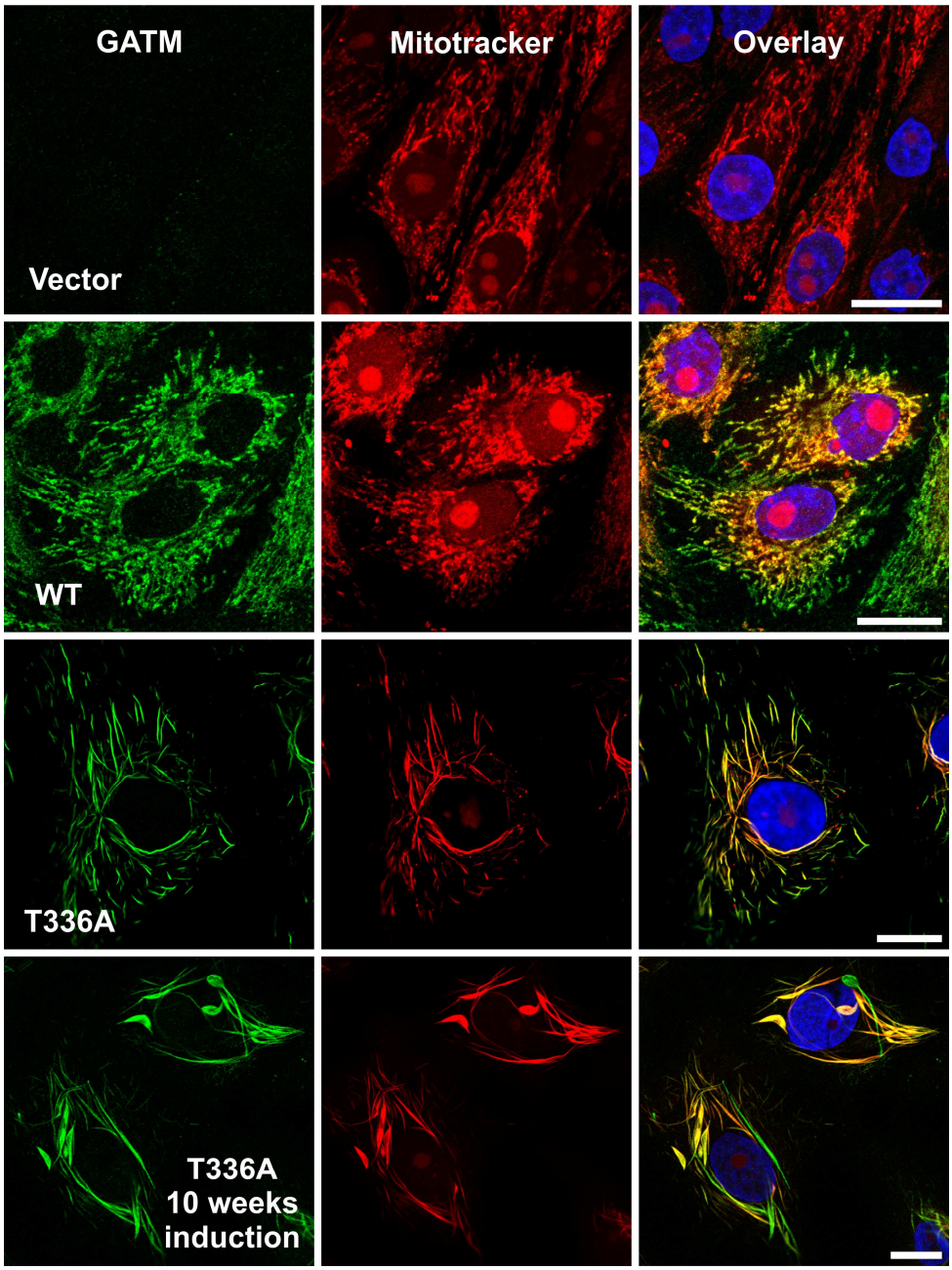

Overexpression of GATM in LLC-PK1 cells: GATM and its mutant form T336A are labeled in green (antibody staining), mitochondria (Mitotracker Orange) in red. Right pictures show overlay images (nuclear staining in blue). Upper panel: Mock transfected LLC-PK1 cells show little to no specific GATM signal. However, it cannot be excluded that the GATM antibody does not bind to endogenous Gatm of porcine LLC-PK1 cells. Second panel: Overexpression of the GATM wildtype protein (overexpression for 3 days). Third panel: T336A mutant (overexpression for 3 days). Fourth panel: Long-term expression of the T336A mutant (overexpression for 10 weeks). Scale bars: 20 µm.

Figure S7

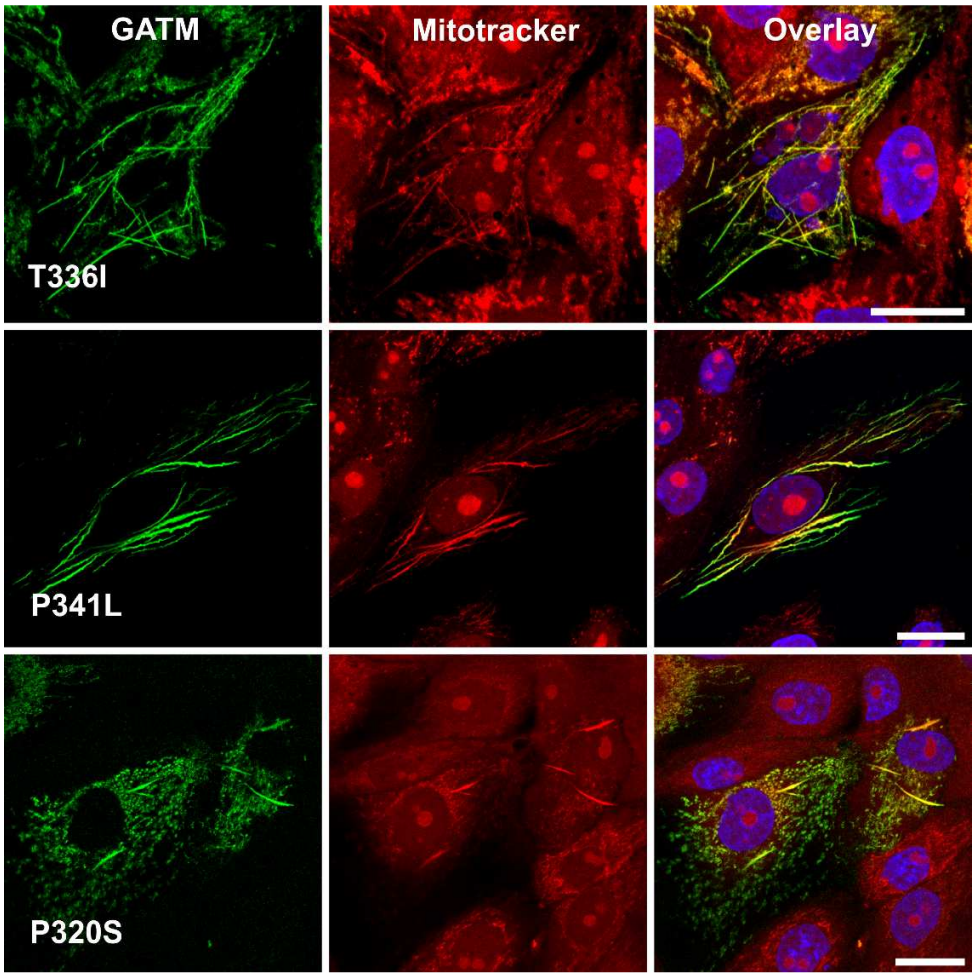

Overexpression of the GATM mutants T336I, P341L, and P320S in LLC-PK1 cells: GATM mutants are labeled in green (antibody staining), mitochondria (Mitotracker Orange) in red. Right pictures show overlay images (nuclear staining in blue). Please note the formation of filaments in cells expressing the mutant forms of GATM. Scale bars: 20 µm.

Figure S8

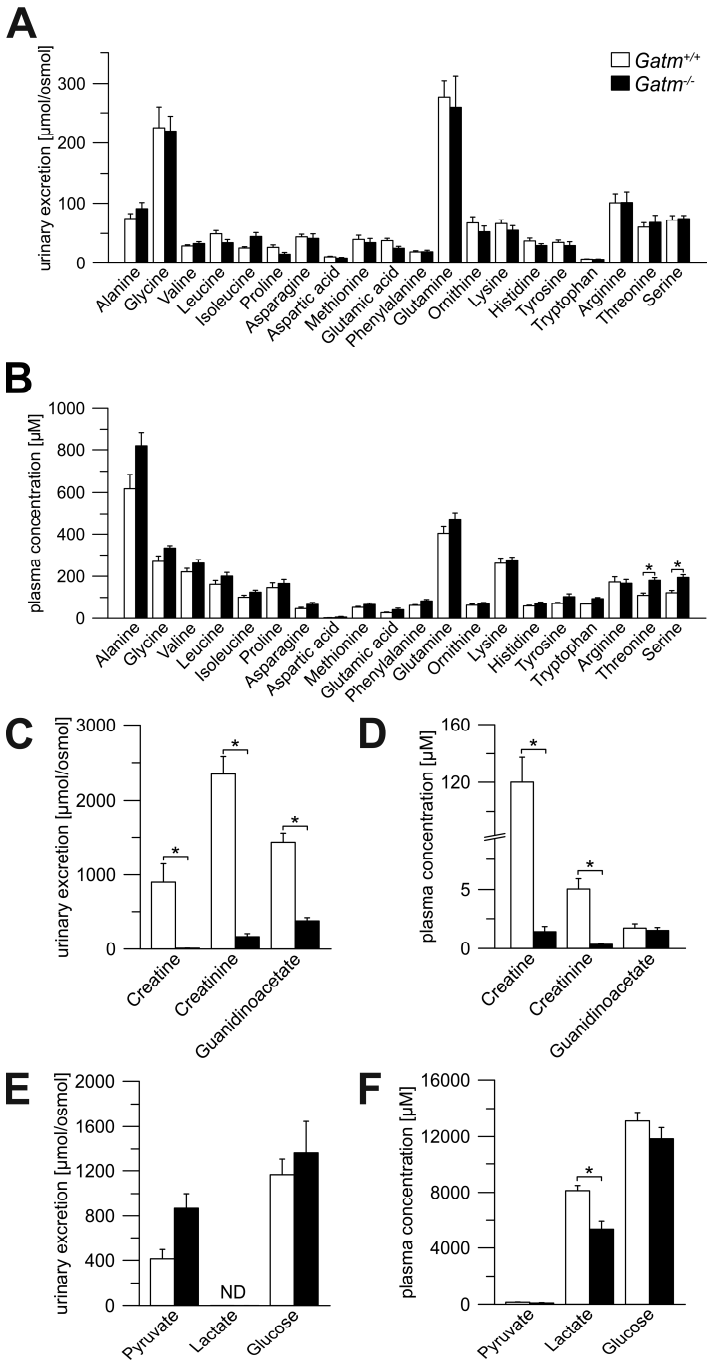

Analysis of urine and plasma from *Gatm*$^{+/+}$ and *Gatm*$^{-/-}$ mice: (A) Urinary excretion of amino acids as well as glucose excretion was not different between *Gatm*$^{+/+}$ and *Gatm*$^{-/-}$ mice (n=6/6, values normalized to osmolyte excretion), which indicates that knockout animals do not suffer from renal Fanconi syndrome. **(B)** In plasma, the concentrations of most amino acids and glucose (non-fasted animals) were similar between the two groups. **(C and D)** As expected, urine and plasma concentrations of creatine and creatinine were

very low in *Gatm*$^{-/-}$ mice, since the endogenous creatine synthesis pathway is disturbed. The residual creatine and creatinine amounts result from creatine absorption from food. Interestingly, the concentration of guanidinoacetate, the direct product of Gatm activity, was normal in plasma whereas the urinary excretion was decreased in knockout mice. **(E)** Urinary excretion of pyruvate, lactate and glucose. **(F)** Plasma concentration of lactate was lower in *Gatm*$^{-/-}$ mice whereas pyruvate concentration was not different. ND = not detectable.

Parameters for LC-MS/MS analysis used in Fig. S8:

Analyte	**Ionization mode**	**Q1 (m/z)**	**Q3 (m/z)**	**Dwell time (ms)**	**DP**
Creatinine	positive –P1	114.0	86.0	150	26
Creatinine d3	positive –P1	117.0	89.0	150	26
Creatine	positive –P1	132.2	90.0	150	21
Guanidinoacetate	positive –P1	118.1	43.0	150	36

DP - declustering potential, P1 - period 1, P2 - period 2

Figure S9

Original Western blot underlying Fig. 4F: Expression of Gatm in response to oral creatine supplementation. Wildtype mice (n=4) were supplemented with 1% creatine in their drinking water for one week (creatine diet), whereas a control group (n=4) received normal tap water (untreated). Afterwards protein expression of Gatm in kidneys was determined using Western blot (upper blot). Values are normalized to β-actin protein expression (lower plot). Quantification of the bands was performed with the software ImageJ.

Figure S10

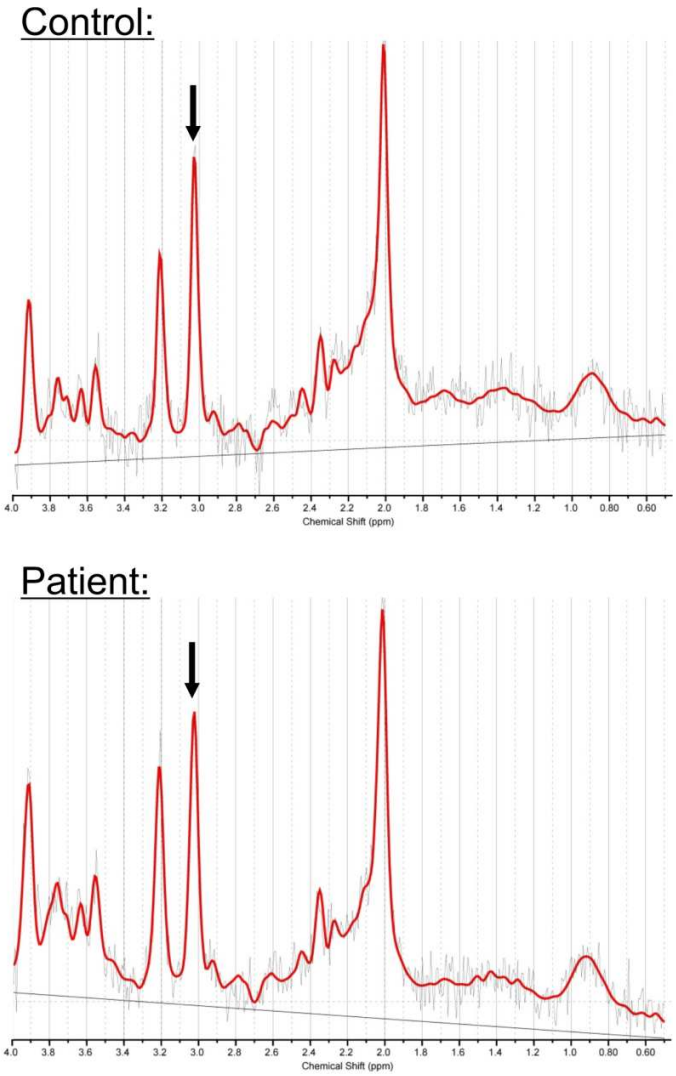

^{1}H-NMR spectroscopy to determine brain (grey matter) creatine content: Note, normal creatine (total) peak (indicated by arrow) in control volunteer (top) and GATM patient (bottom), providing also evidence for GATM's catalytical (i.e. enzymatic) competence. Quantification in the volunteer showed a total creatine of 5.8 mM and 5.0 mM in grey and white matter, respectively. The GATM patient showed 6.1 mM and 4.4 mM in grey and white matter, respectively.

Supplemental Tables

Table S1

Antibodies and conditions for imaging studies. IF: immunofluorescence, WB: Western blot.

Antibody/Dye (Usage)	Species	Dilution	Manufacturer
anti-GATM (IF, WB)	rabbit	1:200 (IF) 1:2000 (WB)	Proteintech, Manchester, UK
anti-α-SMA (IF)	mouse	1:600	Abcam, Cambridge, UK
anti-β-actin (WB)	rabbit	1:5000	Sigma-Aldrich, Taufkirchen, Germany
Alexa Fluor® 555 anti rabbit (IF)	donkey	1:400	Invitrogen, Karlsruhe, Germany
Alexa Fluor® 488 anti mouse (IF)	donkey	1:400	Invitrogen, Karlsruhe, Germany
anti rabbit IgG-HRP (WB)	donkey	1:5000	Santa Cruz, Heidelberg, Germany
MitoTracker Orange CMTMRos (IF) (Stock: 1 mM)		1:5000	Invitrogen, Karlsruhe, Germany
HOE33342 (IF) (Stock: $5x10^{-4}$ M)		1:1000	Invitrogen, Karlsruhe, Germany

Table S2

PCR primer sequences and PCR conditions for expression studies

Gene	Acc. no.	Primer	Sequence (5'>3')	Annealing temp.
murine *GATM*	NM_025961.5	sense	TTTTCAAGAAAGCAGGATGGA	57℃
		antisense	TGACATCCAGAGGGGATGAT	
porcine *FN1*	XM_003133643.2	sense	GAGGCACAAGATTCGGGAGG	61℃
		antisense	CATAATGGGAAACCGTGTAGGG	
porcine *ACTA2*	NM_001164650.1	sense	AGAACACGGCATCATCACCA	61℃
		antisense	CAGGGTCGGATGCTCTTCTG	
porcine *IL-18*	NM_213997	sense	AGCTGAAAACGATGAAGACCTG	61℃
		antisense	AAACACGGCTTGATGTCCCT	
porcine *NLRP3*	NM_001256770	sense	CCTGCAAAAACTGGGGTTGG	60℃
		antisense	CTCCAAGAGCATTTCCCCGT	
porcine *β-actin*	ENSSSCT00000008324	sense	CCCATCTACGAGGGGTACG	60℃
		antisense	CGCTCCGTCAGGATCTTC	
murine *β-actin*	NC_000085.6	sense	GACAGGATGCAGAAGGAGATTACTG	57℃
		antisense	CCACCGATCCACACAGAGTACTT	

Table S3

Laboratory findings of a young patient with GATM-related renal Fanconi syndrome

Substance	Laboratory finding	Age appropriate reference ranges
Plasma values		
Sodium	143 mmol/L	133 - 146 mmol/L
Potassium	3.6 mmol/L	3.5 - 5.5 mmol/L
Chloride	108 mmol/L	100 - 108 mmol/L
Total CO_2	17 mmol/L	20 - 30 mmol/L
Urea	5.3 mmol/L	2.5 - 6.0 mmol/L
Creatinine	22 µmol/L	16 - 33 µmol/L
Calcium	2.47 mmol/L	2.17 - 2.44 mmol/L
Magnesium	0.95 mmol/L	0.66 - 1.00 mmol/L
Phosphate	1.16 mmol/L	1.2 - 2.1 mmol/L
Albumin	49 g/L	34 - 42 g/L
Alkaline Phosphatase (ALP)	413 U/L	145 - 320 U/L
Alanine Transaminase (ALT)	30 U/L	5 - 45 U/L
Total bilirubin	5 µmol/L	< 18 µmol/L
Intact PTH	2.5 pmol/L	0.7 - 5.6 pmol/L
Urine values		
Glucose Stix result	positive +++	negative
Glucose	8.0 mmol/L	
Phosphate	8.86 mmol/L	
Creatinine	0.5 mmol/L	
Phosphate/Creatinine ratio	17.72	1.2 - 14
Tubular Reabsorption of Phosphate	66 %	70 - 100 %
TmP/GFR	0.77 mmol/L	1.10 - 2.70 mmol/L
Urine amino acids		
Glycine/Creatinine ratio	5090 µmol/mmol	250 - 626 µmol/mmol
Serine/Creatinine ratio	2355 µmol/mmol	20 - 100 µmol/mmol
Threonine/Creatinine ratio	2129 µmol/mmol	10 - 45 µmol/mmol
Proline/Creatinine ratio	1864 µmol/mmol	0 - 3 µmol/mmol
Leucine/Creatinine ratio	320 µmol/mmol	3 - 10 µmol/mmol
Isoleucine/Creatinine ratio	141 µmol/mmol	2 - 10 µmol/mmol
Valine/Creatinine ratio	738 µmol/mmol	2 - 8 µmol/mmol
Alanine/Creatinine ratio	3092 µmol/mmol	30 - 80 µmol/mmol
Glutamine/Creatinine ratio	4159 µmol/mmol	30 - 120 µmol/mmol
Arginine/Creatinine ratio	166 µmol/mmol	2 - 10 µmol/mmol
Ornithine/Creatinine ratio	230 µmol/mmol	2 - 10 µmol/mmol
Lysine/Creatinine ratio	1614 µmol/mmol	5 - 30 µmol/mmol
Cystine/Creatinine ratio	226 µmol/mmol	5 - 25 µmol/mmol
Methionine/Creatinine ratio	46 µmol/mmol	3 - 15 µmol/mmol
Taurine/Creatinine ratio	184 µmol/mmol	30 - 105 µmol/mmol
Phenylalanine/Creat ratio	345 µmol/mmol	5 - 15 µmol/mmol
Tyrosine/Creatinine ratio	716 µmol/mmol	5 - 15 µmol/mmol
Tryptophan/Creatinine ratio	193 µmol/mmol	1 - 5 µmol/mmol
Histidine/Creatinine ratio	1909 µmol/mmol	100 - 300 µmol/mmol
Aspartate/Creatinine ratio	82 µmol/mmol	10 - 35 µmol/mmol
Glutamate/Creatinine ratio	86 µmol/mmol	0 - 3 µmol/mmol
Albumin/Creatinine ratio	54.3 mg/mmol	1.5 - 8.7 mg/mmol
NAG/Creatinine ratio	392 U/mmol	2 - 22 U/mmol
Retinol Binding Protein/Creatinine ratio	10420 µg/mmol	2.7 - 103 µg/mmol

Laboratory findings from an affected and genotyped 18 month old child before start of treatment illustrating presence of renal Fanconi syndrome. Note normal plasma creatinine and normal PTH. Note typical signs of renal Fanconi syndrome, i.e. glucosuria, hyperphosphaturia and hypophosphatemia, generalized hyperaminoaciduria, low molecular weight proteinuria, metabolic acidosis and slightly elevated alkaline phosphatase (in red).

References

1. Joncquel-Chevalier, CM, Voicu, PM, Fontaine, M, Dessein, AF, Porchet, N, Mention-Mulliez, K, et al.: Creatine biosynthesis and transport in health and disease. *Biochimie,* 119**:** 146-165, 2015.
2. Engelke, U, Moolenaar, S, Hoenderop, S, Morava, E, van der Graaf, M, Heerschap, A, et al.: *Handbook of 1H-NMR spectroscopy in inborn errors of metabolism: body fluid NMR spectroscopy and in vivo MR spectroscopy,* Heilbronn, SPS Verlagsgesellschaft, 2007.
3. Klootwijk, ED, Reichold, M, Helip-Wooley, A, Tolaymat, A, Broeker, C, Robinette, SL, et al.: Mistargeting of peroxisomal EHHADH and inherited renal Fanconi's syndrome. *N Engl J Med,* 370**:** 129-138, 2014.
4. van der Goot, AT, Zhu, W, Vazquez-Manrique, RP, Seinstra, RI, Dettmer, K, Michels, H, et al.: Delaying aging and the aging-associated decline in protein homeostasis by inhibition of tryptophan degradation. *Proc Natl Acad Sci U S A,* 109**:** 14912-14917, 2012.